Biophysical Journal Volume 73 August 1997 770–778

Intrinsic Rectification of Ion Flux in Alamethicin Channels: Studies with an Alamethicin Dimer

G. Andrew Woolley,* Philip C. Biggin,# Aylit Schultz,* Linda Lien,* Dominic C. J. Jaikaran,* Jason Breed,# Karin Crowhurst,* and Mark S. P. Sansom#

*Department of Chemistry, University of Toronto, Toronto M5S 3H6, Canada, and #Laboratory of Molecular Biophysics, University of Oxford, Oxford OX1 3QU, England

ABSTRACT Covalent dimers of alamethicin form conducting structures with gating properties that permit measurement of current-voltage (*I-V*) relationships during the lifetime of a single channel. These *I-V* curves demonstrate that the alamethicin channel is a rectifier that passes current preferentially, with voltages of the same sign as that of the voltage that induced opening of the channel. The degree of rectification depends on the salt concentration; single-channel *I-V* relationships become almost linear in 3 M potassium chloride. These properties may be qualitatively understood by using Poisson-Nernst-Planck theory and a modeled structure of the alamethicin pore.

INTRODUCTION

Alamethicin channels are formed by self-assembly of several bent α-helical monomers into a helix-bundle structure that traverses the membrane (Cafiso, 1994; Sansom, 1993b; Woolley and Wallace, 1992). This architecture is similar to that of the transmembrane region of the acetylcholine receptor channel, where the pore is composed of a bundle of five bent α-helices (Unwin, 1995; Breed et al., 1996). The relatively small size of alamethicin channels makes detailed biophysical and structural studies possible. This peptide can therefore serve as a model for developing a molecular understanding of ion transport in helix-bundle channels.

Macroscopic (many-channel) current-voltage (*I-V*) relationships of alamethicin and analogs have been characterized in detail. These relationships reflect primarily the voltage dependence of channel formation rather than the conductance properties of individual alamethicin channels (Gordon, 1973; Latorre and Alvarez, 1981). Because the alamethicin channel is a dynamic structure that can change size abruptly by the attachment or departure of a peptide monomer, it has been difficult to characterize the single-channel *I-V* properties of individual conducting states. The lifetime of any one state is generally shorter than the time required to measure a single-channel *I-V* relationship by applying a voltage ramp. As a result, the single-channel *I-V* relationships that have been reported are composites obtained by measuring current amplitudes of single channels at a series of holding potentials (Boheim et al., 1983; Gordon and Haydon, 1972; Mak and Webb, 1995b; Taylor and de Levie, 1991).

If alamethicin is present at one side of the membrane only, channels will generally only form when the voltage is held positive on that side (Vodyanoy et al., 1983). If peptide molecules can traverse the membrane, or if they are already present at both sides of the membrane, they will insert from whichever side of the membrane is held positive (Vodyanoy et al., 1983). Thus channels either do not open with *cis*-negative holding potentials or, in the case where peptide is present on both sides of the membrane, channels that open at *cis*-negative potentials will behave in the same manner as their symmetry-related equivalents, which open at *cis*-positive potentials. Only one limb of the *I-V* relationship is thus readily accessible. The negative limb of the curve measured in the above manner provides no new information regarding the properties of the pore; it is simply the positive limb inverted through the origin (0,0). In the absence of information about the *I-V* relation in the third quadrant, simple single-barrier models have been developed to describe ion transport and noise properties of alamethicin channels (Mak and Webb, 1995a,b). Such models produce *I-V* curves that are symmetrical about the origin.

Recently we described the covalent dimerization of alamethicin (Rf50) molecules, which led to the stabilization of a particular conducting state (You et al., 1996). The lifetime of this state is sufficient to make possible a full *I-V* measurement by applying a voltage ramp. This measurement clearly demonstrates that the *I-V* relationship of an alamethicin channel is intrinsically asymmetrical with respect to the origin, as had been suggested by previous measurements of alamethicin (Rf30) current transients (Boheim et al., 1983; Taylor and de Levie, 1991), as well as by the behavior of related synthetic channel-forming peptides (Kienker et al., 1994; Kienker and Lear, 1995). Moreover, the degree of rectification is dependent on the potassium chloride concentration of the solutions employed; the asymmetry is less pronounced at higher salt concentrations. These observations can be qualitatively understood in terms of continuum electrostatic theory and a detailed (modeled) structure of the alamethicin pore.

Received for publication 8 January 1997 and in final form 22 April 1997.

Address reprint requests to Dr. Andrew Woolley, Department of Chemistry, University of Toronto, 80 St. George St., Toronto, ON M5S 3H6, Canada. Tel.: 416-978-0675; Fax: 416-978-8775; E-mail: awoolley@chem.utoronto.ca.

© 1997 by the Biophysical Society

0006-3495/97/08/770/09 $2.00

MATERIALS AND METHODS

Diphytanoyl-*sn*-glycero-3-phosphatidylcholine was purchased from Avanti Polar Lipids. All other chemicals were obtained from Sigma/Aldrich and were the highest grade available. Alamethicin-bis(*N*-3-aminopropyl)-1,7-heptanediamide (ala-BAPHDA), a covalent dimer of alamethicin Rf50, was synthesized and purified as described previously (You et al., 1996).

Single-channel measurements

Peptides (~0.1 μM in methanol) were added to both sides of membranes formed from diphytanoyl phosphatidylcholine/decane (50 mg/ml), using established techniques (Seoh and Busath, 1993). Potassium chloride (KCl) solutions (at the concentrations indicated in figure legends) were buffered with *N,N*-bis(2-hydroxyethyl)-2-aminoethanesulfonic acid (BES) (5 mM) to pH 6.8, and all measurements were made at 22°C (±2°C). The addition of EDTA (2 mM) had no effect on the measured currents. Currents were measured and voltage was set with an Axopatch 1D patch-clamp amplifier (Axon Instruments) controlled by Synapse (Synergistic Research Systems) software. Data were filtered at either 2 kHz or 1 kHz, sampled at 5× the filter frequency, stored directly to disk, and analyzed with Synapse and Igor (Wavemetrics) software. Single-channel current-voltage (*I-V*) curves were obtained by using the following voltage-clamp protocol: a step from 0 mV to 200 mV, holding at 200 mV for 50 to 500 ms, then a ramp to −200 mV over the course of 10–50 ms, followed by a return to 0 mV for several seconds. Capacitive currents obtained when no channel opened were subtracted from currents obtained with a single channel open during the ramp. Data shown are for individual ramps. Repeat ramps (generally 5–25) gave *I-V* curves that were superimposable on those shown. *I-V* curves were obtained for channels opening at −200 mV by applying an inverted protocol (i.e., a ramp from −200 to +200 mV). Slope conductances were obtained by fitting polynomials to the measured current and voltage values (using the data analysis program Igor; Wavemetrics), differentiating the polynomials, and dividing the result. The slope conductance was normalized by dividing it by the salt concentration; the results were then plotted versus voltage (Fig. 4 *C*).

Calculation of electrostatic energy profiles

Calculations were performed on the hexameric structure shown in Fig. 1, which is representative of an ensemble of 25 hexamer models. As discussed below, the molecularity of the channel is not unambiguously known, but a hexamer is the minimum structure that can account for the observed properties. Calculations have been performed on larger and smaller bundles, and qualitatively similar results have been obtained. All data were calculated using University of Houston Brownian Dynamics to solve the linearized Poisson-Boltzmann equation (Davis et al., 1991). The alm-BAPHDA bundle was positioned in a low-dielectric (ϵ = 2) slab 32.5 Å thick to mimic the presence of a lipid bilayer, as indicated in Fig. 1 *B*. The protein was also assigned a dielectric of ϵ = 2. The ends of the channel were bathed in slabs of dielectric ϵ = 78 (~13 Å on each side) to represent bulk solvent. The region within the pore was also assigned a dielectric of ϵ = 78.

The grid spacing was 1 Å, and a 58 × 58 × 58 grid was used. A smaller grid spacing did not seem warranted because the root mean squared deviation of backbone atoms in the ensemble of bundle structures was 1.7 Å (Breed et al., 1997). Partial charges and radii were taken from the CHARMm22 parameter set. A temperature of 300 K was used for all simulations, and the ionic strength was set as indicated in the figure legends. The Stern radius was set at 2 Å, so that counterions would be able to penetrate all but the very narrowest region of the pore. Counterions are mainly present in the slabs of bulk solution bathing the channel ends. Electrostatic potential profiles were obtained by calculating the energy of a +1*e* probe charge at successive positions along the center of the pore, as defined by HOLE (Smart et al., 1993) calculations of the pore radius profile.

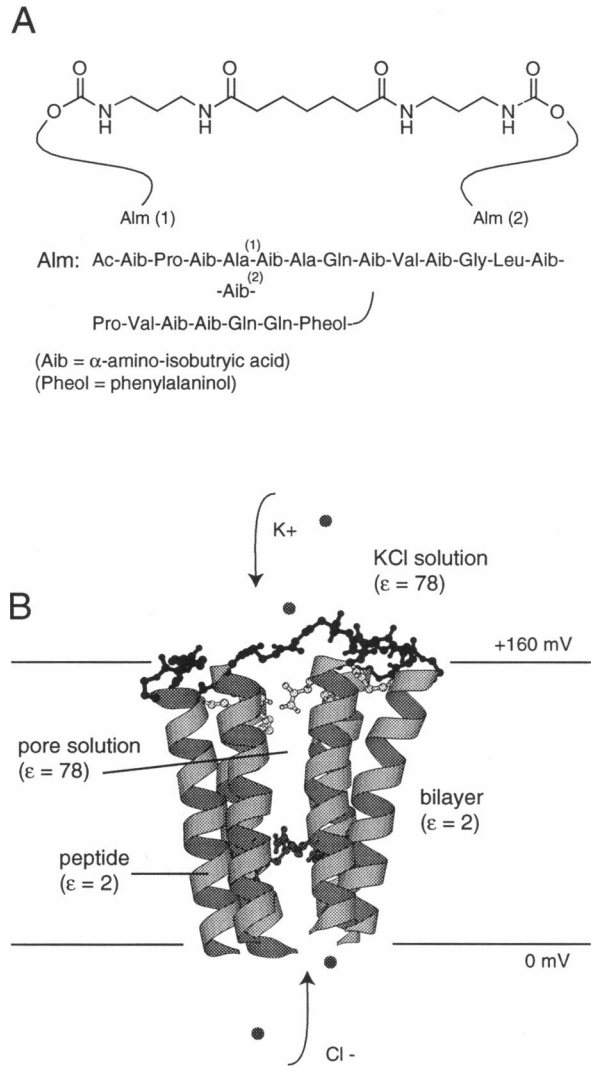

FIGURE 1 (*A*) Primary structure of alamethicin-BAPHDA dimer. (*B*) Side view of a model of the alamethicin-BAPHDA channel structure generated as described by You et al. (1996). The molecularity of the structure has not been unambiguously determined, but the hexameric (three-dimer) structure shown is the minimum size consistent with the experimental data. The backbones of the alamethicin monomers are represented by ribbons. The linkers are in black and connect the C-terminal ends of the monomers. The Gln[18] (*light grey*) and Gln[7] (*dark grey*) side chains are shown. With an applied voltage as shown, cations enter the C-terminal end and anions enter the N-terminal end of the channel.

Calculation of *I-V* curves

If one assumes the fluxes of anions and cations to be independent (see below), total current through the channel may be calculated by using Nernst-Planck theory (Schultz, 1980; Hille, 1992):

$$I_{\text{total}} = [C]A\left(\left(-z_c F\beta_c \frac{\exp(z_c F\psi_c/RT) - 1}{\int_0^l [\exp(z_c F\psi_{xc}/RT)/D_c]\mathrm{d}x}\right) + \left(-z_a F\beta_a \frac{\exp(z_a F\psi_a/RT) - 1}{\int_0^l [\exp(z_a F\psi_{xa}/RT)/D_a]\mathrm{d}x}\right)\right) \quad (1)$$

where [*C*] is the salt activity (equal on both sides of the membrane; activity coefficients were taken from the *CRC Handbook of Chemistry and Physics*,

61st Ed.); A is the cross-sectional area (see below); z_c is the cation valence (+1); β_c is the partition coefficient for cations from the bulk solution into the channel; D_c is the diffusion coefficient for cations within the channel; z_a, β_a, and D_a are the corresponding quantities for anions; F is the Faraday constant; R is the gas constant; and T is the absolute temperature. ψ_x is the potential at position x in the membrane, ψ is the applied potential (subscripts denote whether these potentials are for cations or anions). The integral was taken over the effective length of the channel (l), which was chosen so that the electrostatic energy of a test charge was zero at each end in the absence of an applied potential (l varied with ionic strength; Fig. 8 A). Because little is known about how the effective diffusion coefficients vary in the pore (see Discussion), and because we did not wish to dictate a selectivity for cations or anions, D_a and D_c were assumed to be constant, and equal for K^+ and Cl^- (i.e., $D_a = D_c = D$), and $\beta_c = \beta_a = \beta$. With these assumptions, Eq. 1 can be simplified as follows:

$$I_{\text{total}} = FD\beta[C]A\left(\left(-\frac{\exp(z_cF\psi_c/RT) - 1}{\int_0^l [\exp(z_cF\psi_{xc}/RT)]\mathrm{d}x}\right) + \left(\frac{\exp(z_aF\psi_a/RT) - 1}{\int_0^l [\exp(z_aF\psi_{xa}/RT)]\mathrm{d}x}\right)\right) \quad (2)$$

The term

$$\int_0^l [\exp(z_cF\psi_{xc}/RT)]\mathrm{d}x \quad (3)$$

which describes how the electrostatic potential varies through the pore, was represented as a sum of two terms, i.e.,

$$\int_0^l \left[\exp\left(z_cF\left(\frac{\psi_c x}{l} + kf_c(x)\right)/RT\right)\right]\mathrm{d}x \quad (4)$$

where $f_c(x)$ is the polynomial fit to the electrostatic potential profile for cations calculated above (Fig. 8 A). The factor k was inserted to permit weighting of the magnitude of this electrostatic profile relative to the applied field. Importantly, the same value of k (= 0.5) was used for all ionic strengths; thus relative differences in the calculated profiles will determine relative differences in the I-V curves. If $k = 0$, the voltage drops linearly across the membrane and a linear I-V relationship is obtained, as expected, because the salt concentration is the same on both sides of the membrane (Schultz, 1980). A term analogous to Eq. 4 was used for anions, where $f_a(x)$ was simply $-f_c(x)$. Combining these expressions gives

$$I_{\text{total}} = FD\beta[C]A\left(\left(-\frac{\exp(z_cF\psi_c/RT) - 1}{\int_0^l [\exp(z_cF((\psi_c x/l) + kf_c(x))/RT)]\mathrm{d}x}\right) + \left(\frac{\exp(z_aF\psi_a/RT) - 1}{\int_0^l [\exp(z_aF((\psi_a x/l) + kf_a(x))/RT)]\mathrm{d}x}\right)\right) \quad (5)$$

Using a value for D of 2×10^{-5} cm^2 s^{-1} (the value for K^+ or Cl^-) in aqueous solution (Hille, 1992), $\beta = 1$, and a cross-sectional area of 32 Å^2 (estimated so that the volume of the channel calculated from the model structure using the program HOLE (Smart et al., 1993) (i.e., 1277 Å^3) is the same as that of a simple cylinder with l = 40 Å and area 32 Å^2), the single-channel current (in pA) is given by

$$I_{\text{calc}}(\text{pA}) = 0.617[C] \cdot \left(\left(-\frac{\exp(z_cF\psi_c/RT) - 1}{\int_0^l [\exp(z_cF((\psi_c x/l) + kf_c(x))/RT)]\mathrm{d}x}\right) + \left(\frac{\exp(z_aF\psi_a/RT) - 1}{\int_0^l [\exp(z_aF((\psi_a x/l) + kf_a(x))/RT)]\mathrm{d}x}\right)\right) \quad (6)$$

where $[C]$ is in mM and l is in Å. This expression was integrated numerically using Mathematica (Wolfram Research) for a range of ψ from −200 mV to +200 mV to produce calculated I-V curves. Finally, a single parameter was used to multiply the calculated current to best fit the observed current (Fig. 8 B), i.e.,

$$I_{\text{fit}}(\text{pA}) = cI_{\text{calc}} \quad (7)$$

Again, this parameter was the same for all ionic strengths. The numerical value of c turned out to be ~1.32, a rather small correction, considering the simplicity of the model (see Discussion).

RESULTS AND DISCUSSION

Rectifying single-channel *I-V* curves

A channel formed by alamethicin dimers is shown schematically in Fig. 1. Dimers are composed of monomers linked at their C-termini. N-terminal insertion of the peptides leads to an all-parallel arrangement of helices in the channel, with the C-terminal end at the positive side of the membrane. Evidence for this mode of insertion comes from studies on the behavior of chemically modified (C-terminally and N-terminally charged) alamethicin analogs (Hall et al., 1984; Woolley et al., 1994), and from NMR and electron paramagnetic resonance studies of alamethicin in bilayer membranes (Barranger-Mathys and Cafiso, 1996; North et al., 1995), and is supported by simulation studies (Biggin et al., 1997). The physical origin of this orientational preference appears to be the helix macro-dipole of the peptide (see below).

The channel passes both cations and anions (Hall et al., 1984), so that with the applied voltage as shown, K^+ ions enter the C-terminal end and Cl^- ions enter the N-terminal end of the channel. With a negative applied voltage, the same channel will form from the other side of the membrane (because peptide is present at both sides of the membrane in these experiments) and will have exactly the same characteristics. The structure shown contains six peptide molecules (three dimers). The evidence for this is reviewed in You et al. (1996), but the molecularity of the structure is not unambiguously known. The molecularity does not substantially affect the present qualitative analysis, except for the fact that the calculated magnitude of the ionic strength effect would be different for a larger structure (see below).

A single-channel current-voltage (I-V) relationship obtained with alamethicin-BAPHDA in 1 M KCl is shown in Fig. 2. Two curves are shown: one is obtained by starting with a holding potential of +200 mV and applying a voltage ramp to −200 mV (the channel closes at about −140 mV); the second is obtained by starting with a holding potential of −200 mV and applying a ramp to +200 mV (the channel closes at about +160 mV). These two curves are related through a center of symmetry at (0,0). If the absolute values of the current and voltage are taken, these two curves are superimposable. This is expected, if the same structure is forming from either side of the membrane. Any one curve, however, is distinctly asymmetrical with respect to the origin. The current measured when the voltage has the same

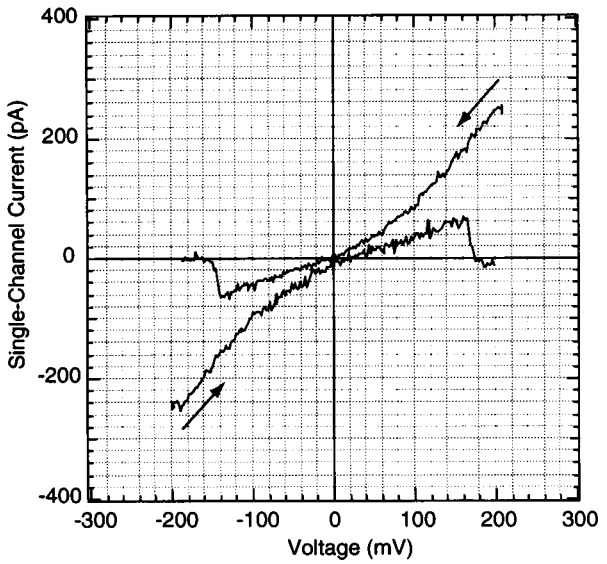

FIGURE 2 Single-channel current-voltage curve for the alamethicin-BAPHDA channel in 1 M KCl, 5 mM BES, 2 mM EDTA, pH 6.8. In the upper curve, a channel opened with a holding potential of +200 mV and stayed open during a voltage ramp to approximately −140 mV, where it closed abruptly (transition to zero current). The direction of the voltage ramp is indicated by the arrow. In the lower curve, a channel opened with a holding potential of −200 mV and stayed open during a voltage ramp to approximately +160 mV. The capacitive current of the membrane without an open channel has been subtracted in each case.

sign as it did when the channel opened is significantly larger than that measured when the voltage has the opposite sign.

The chance of a channel closing appears to increase toward the end of the voltage ramp, because it was difficult to obtain recordings significantly past −100 mV (or +100 mV for the opposite ramp). Presumably, toward the end of the ramp, the voltage acts to reorient the peptide helix dipoles. Once a channel closes (at −140 mV, for instance) a channel of the same conductance does not form again unless a ramp is begun again (i.e., from +200 mV).

Because no current transition is observed during the ramp, except where the channel closes, one must conclude that the current measured corresponds to current flowing through a structure that does not "flip" orientation with respect to the membrane (a structural transition might occur at zero current, but would have to happen only there, consistently, not to be observed). These results therefore demonstrate that ion movement opposite the direction shown in Fig. 1 (i.e., K^+ ions moving from the N-terminal end to the C-terminal end of the channel and Cl^- ions vice versa) is significantly less facile than the normal orientation.

This observation of rectification by alamethicin-BAPHDA channels is consistent with the observation reported by Boheim (1983) and by Taylor and de Levie (1991), that, in certain cases, single-channel currents measured immediately after a voltage reversal were significantly smaller than those measured before. The currents reported by these authors were transient; they rapidly underwent transitions to lower conductance states and closed. One could not be sure that the abrupt voltage reversal in these experiments did not cause a structural transition of some sort (e.g., a helix flip-flop) that would account for the smaller currents; such a transition would have been obscured by the large capacitive transient. Indeed, Taylor and de Levie reported that a voltage reversal sometimes did cause qualitatively different channel behavior (Taylor and de Levie, 1991).

The presence of the linker in alm-BAPHDA does not appear to affect the pore properties of these channels per se, because the positive limbs of the *I-V* curves of alm-BAPHDA and alamethicin Rf50 monomers (in the corresponding conducting state) are superimposable (You et al., 1996).

Rectifying single-channel *I-V* curves similar to those observed here have recently been reported for an uncharged synthetic channel-forming peptide: $Ac(LSSLLSL)_3$-$CONH_2$ (Kienker et al., 1994; Kienker and Lear, 1995). This peptide appears to form channels in a manner similar to that of alamethicin, i.e., through self-assembly of a parallel bundle of helices, although the detailed channel structure is substantially different.

Thus alm-BAPHDA, alamethicin Rf50 monomers, alamethicin Rf30 monomers (studied by Taylor and de Levie, 1991), and the peptides studied by Kienker and Lear (1995) all show qualitatively similar behavior. Intrinsic rectification is therefore likely to be a general property of parallel helix-bundle channels.

Effects of varying the KCl concentration

To probe the origins of this intrinsic rectification, we performed a series of experiments using different concentrations of potassium chloride (KCl).

Fig. 3 shows single-channel records of alamethicin-BAPHDA at several different KCl concentrations. Dimerization does not completely remove the different conductance states traditionally observed with alamethicin, but does greatly restrict their number. One predominant conducting state is consistently observed at a variety of salt concentrations. The presence of other (short-lived) conductance states, in fact, provides a convenient reference which indicates that the same structure is being formed with different KCl concentrations: subconductance transitions during the lifetime of the main conducting state (and at the beginning and end of the channel event) remain at a constant fraction of the main conductance as the KCl concentration is varied (Fig. 3).

Single-channel *I-V* curves were also recorded at a range of salt concentrations (by applying voltage ramps as described). Fig. 4 shows a comparison of *I-V* curves obtained with 3 M KCl (Fig. 4 *A*) and 0.5 M KCl (Fig. 4 *B*). The 3 M KCl record is distinctly more linear than that obtained with 0.5 M KCl; a quantitative measure of this effect is obtained by calculating the slope conductance (normalized by dividing by the salt concentration) and plotting this

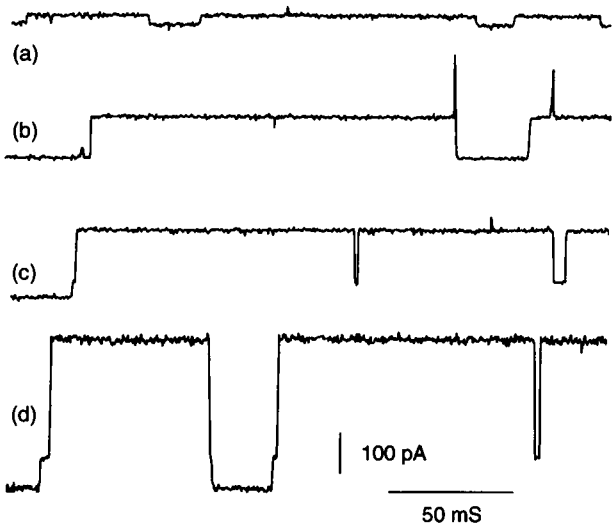

FIGURE 3 Single-channel records of alamethicin-BAPHDA channels at different KCl concentrations. All records are with an applied voltage of +160 mV; solutions contained 5 mM BES, pH 6.8. (*a*) 0.1 M, (*b*) 0.5 M, (*c*) 1 M, (*d*) 2 M KCl.

versus voltage (Fig. 4 *C*). The asymmetry of the 0.5 M curve with respect to zero voltage is considerably more pronounced than that of the 3 M curve. The 1 M curve is intermediate.

Data for a more extensive range of salt concentrations are presented in Fig. 5. The observed current for a range of voltages is plotted versus potassium chloride concentration. Currents are consistently smaller with a "reversed" voltage (Fig. 5 *B*) than with a "normal" voltage (Fig. 5 *A*). There is no clear evidence of saturation, even with 3 M KCl, except perhaps with the lowest voltages (25 mV, Fig. 5 *A*). The slight curvature toward the KCl concentration axis in Fig. 5 *A* is similar to that observed when the conductances of KCl (bulk) solutions are plotted versus KCl concentration. The unusual upward curvature observed with "reversed" voltages (Fig. 5 *B*) in the range of 0–2 M KCl is a direct consequence of the change in the curvature of the *I-V* plots with salt concentration.

An electrostatic model of the channel

Detailed molecular models of the alamethicin pore have been developed by the technique of molecular dynamics with simulated annealing (Breed et al., 1997; Breed and Sansom, 1994; Kerr et al., 1994; You et al., 1996). These models take into consideration all structural data on the pore in membranes. Ideally, one could use these models to attempt to describe the observed ion flux quantitatively in terms of theories of ion permeation (Bek and Jakobsson, 1994; Cooper et al., 1985). However, because there is limited information about the molecularity of the conducting structure, it seems premature to develop complete descriptions that attempt to match experimental *I-V* relationships quantitatively. Instead, we wish to determine whether

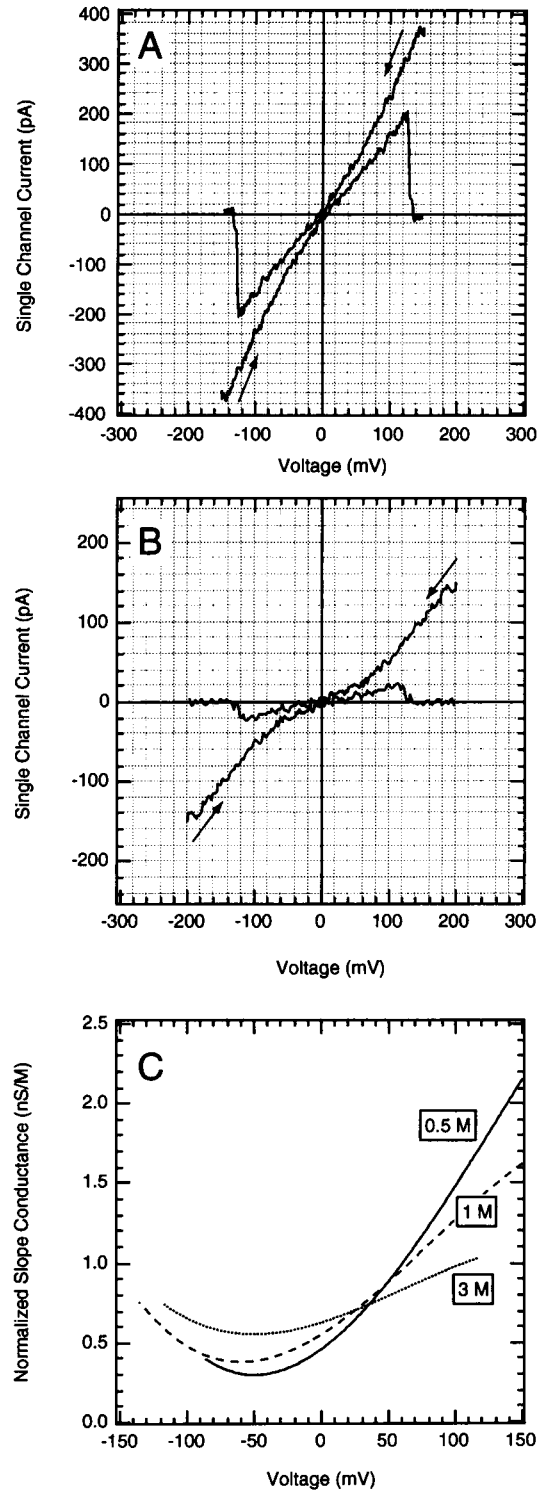

FIGURE 4 Single-channel current-voltage curve for the alamethicin-BAPHDA channel in (*A*) 3 M KCl, (*B*) 0.5 M KCl. Other conditions were as in Fig. 2. Typically 5–20 ramps were obtained with both positive and negative holding potentials, and these were found to be nearly superimposable. For clarity, only one ramp and its reflection through the origin is shown. In each case the direction of the voltage ramp is indicated by the arrow. (*C*) Normalized slope conductance of alamethicin-BAPHDA channels versus voltage at different KCl concentrations: 0.5 M (——), 1 M (– – –), 3 M (·····).

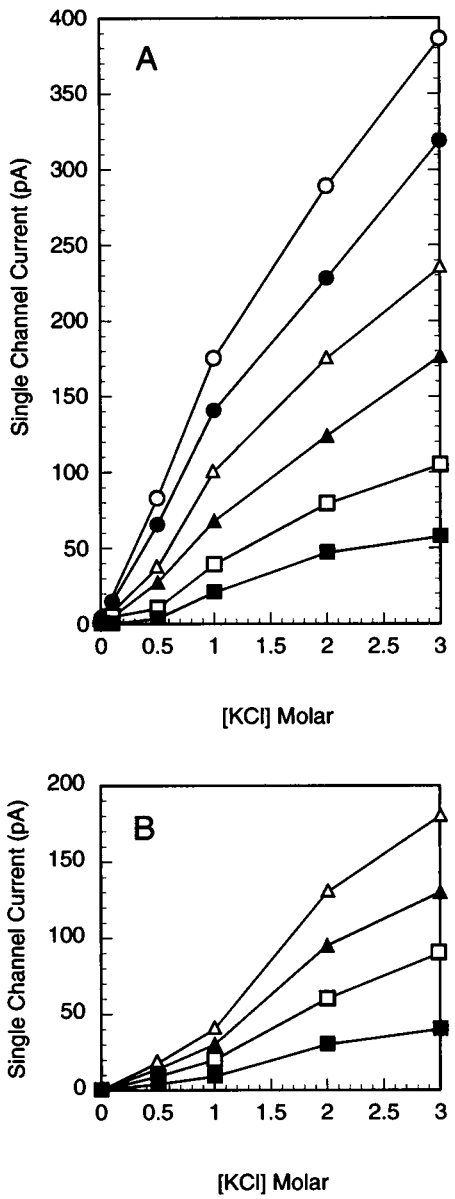

FIGURE 5 Single-channel current versus KCl concentration at a series of different voltages. (*A*) Voltage of the same sign as the initial holding potential. (*B*) Voltage of the opposite sign that of the initial holding potential. Voltages were 25 mV (■), 50 mV (□), 75 mV (▲), 100 mV (△), 125 mV (●), and 150 mV (○).

the models can provide a qualitative explanation for the observed single-channel rectification and its dependence on salt concentration. We assume from the outset that voltage changes do not affect the conformation of the open pore; the validity of this assumption is not known.

The alamethicin-BAPHDA structure has no formal charges, and the lack of an effect of the divalent ion chelator EDTA on channel currents indicates that divalent ions are not responsible for the observed rectification. The directional preference for ion flow must therefore arise as a consequence of the structure and partial charge distribution of the channel itself. Several lines of evidence indicate that the secondary structure of the alamethicin channel is predominantly helical (Woolley and Wallace, 1992). The α-helix has a significant dipole moment due to alignment of the peptide bond dipoles in the structure. This dipole is oriented approximately along the helix axis, such that the positive end is at the N-terminus and the negative end is at the C-terminus. Indeed, it is this dipole moment that is believed to be responsible for the voltage dependence of channel formation by alamethicin; it favors N-terminal insertion of alamethicin when a *cis*-positive voltage is applied (Sansom, 1993a; Biggin et al., 1997; Hall et al., 1984).

However, the structure of the alamethicin pore is not simply a bundle of parallel straight helices with their dipole moments aligned perpendicular to the membrane surface. The structure shown in Fig. 1 is representative of a family of related structures calculated by using molecular dynamics/simulated annealing. As a family, these structures have several common features. The bend in the helix axis around Pro^{14} leads to a funnel-shaped pore with a wider diameter at the C-terminal end than at the N-terminus. The narrowest region is at the level of the Gln7 residues, which may form an intermolecular ring of hydrogen bonds (Molle et al., 1996).

An estimate of the electrostatic energy profile of a cation (or anion) in the pore can be made by numerically solving the Poisson-Boltzmann equation as a test ion is moved through the model. This calculation takes into account the detailed distribution of fixed charge in the channel (e.g., the peptide dipoles) as well as the different dielectric environments present in the system. For simplicity, we divide the system into two dielectric regions: that of the peptide and surrounding lipid slab, and that of the bulk solution and aqueous pore (see diagram in Fig. 1). A dielectric constant (ϵ) of 78 was assumed for bulk solution. The effective dielectric constant in the pore may be lower than this (see Gutman et al., 1992), but to subdivide the aqueous pore and bulk solvent regions poses computational problems with our current procedures. A dielectric constant of 2 was initially assumed for the peptide and lipid region.

Fig. 6 shows calculated electrostatic profiles for a cation in the modeled pore. The solid lines in Fig. 6, *A* and *B*, are calculated assuming ϵ(peptide) = 2, ϵ(solution) = 78, and an ionic strength of 0.1 M. Other curves show the effect of varying the dielectric constant. In all cases, a pronounced asymmetry is evident; the electrostatic energy of a cation is significantly lower at the C-terminal end of the channel than it is at the N-terminal end (and so, conversely, for anions). In addition, the profiles are not centrosymmetrical, because the wells are larger than the peaks. In Fig. 6 *A* the solution and pore dielectric constant are varied with ϵ(peptide) = 2. In Fig. 6 *B* the peptide/lipid dielectric constant is varied with ϵ(solution) = 78. The choice of dielectric constant appears to affect primarily the magnitude of the calculated electrostatic potential. Although the detailed shapes of the curves change with different values of ϵ, the overall asymmetry is preserved. In applying these calculated electrostatic profiles to a description of ion flux through the channel, we there-

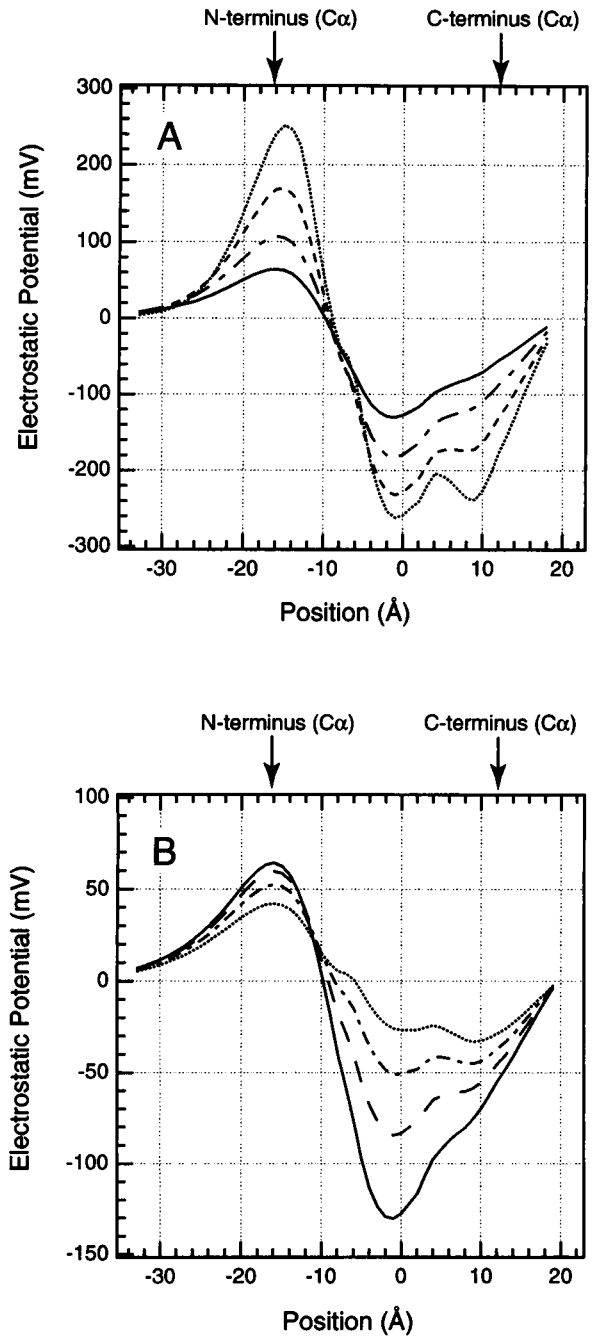

FIGURE 6 Effects of different dielectric constants on calculated electrostatic potential profiles for a cation as it moves through the pore (see Materials and Methods). The zero position is the z coordinate of the center of mass of the channel; the average positions of the α-carbon atoms at the channel termini are indicated. (*A*) Profiles calculated for a peptide/lipid dielectric of 2 and solution dielectrics of 78 (——), 40 (– · –), 20 (– – –), and 10 (·····). (*B*) Profiles calculated for a solution dielectric of 78 and peptide/lipid dielectrics of 2 (——), 6 (– – –), 15 (– · –), and 40 (·····). The ionic strength was 0.1 M.

fore allow an empirical correction factor to scale the magnitude of the electrostatic profile (see below).

Fig. 7 shows calculated electrostatic profiles for a series of different ionic strengths (using ϵ(peptide) = 2, ϵ(solution) = 78). As the ionic strength increases, the magnitudes of the calculated electrostatic energies decrease significantly, consistent with shielding of channel charge.

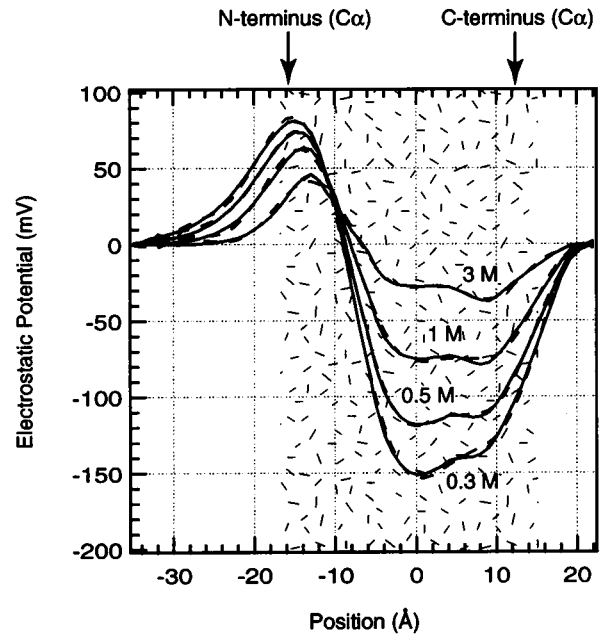

FIGURE 7 Electrostatic potential of a cation versus distance through the pore as a function of ionic strength (see Materials and Methods). The zero position is the z coordinate of the center of mass of the channel; the average positions of the α-carbon atoms at the channel termini are indicated. The stippled region represents the lipid bilayer slab. The dashed curves are fitted polynomials (15th order). The potential of an anion was taken as the negative of this profile.

Description of the observed currents in continuum-theory terms

Although the pore appears to have a relatively narrow region formed by the ring of Gln[7] residues (Molle et al., 1996; Sansom, 1993a), it is not clear that this region provides an energy barrier sufficiently sharp to distinguish it from other regions of the channel—a starting point for rate-theory approaches to describing ion flux (Levitt, 1986; Begenisich, 1994). Description of ion transport in terms of "bidirectional thermally activated transport of ions over a single energy barrier inside the channel" (Mak and Webb, 1995a,b) (e.g., the Gln7 ring) is inadequate, because this treatment leads to symmetrical *I-V* curves, contrary to what is observed (Figs. 2 and 4).

A continuum approach has been developed by Levitt to describe ion flux through acetylcholine receptor channels (Levitt, 1991a,b). These channels appear to be structurally similar to the alamethicin channels described here, except that the acetylcholine channels contain fixed charges in the pore. The presence of a dipole could presumably be mimicked by appropriately placed fixed charges. Levitt predicts rectifying *I-V* relationships like those described here when a fixed charge is at one end of the pore. Moreover, the degree

of rectification goes down as the ionic strength is raised (Levitt, 1985).

Continuum theory and barrier models have been used to attempt to explain the conductance and selectivity of the synthetic channel-forming peptides studied by Kienker and Lear (1995). A Poisson-Nernst Planck approach was reported to provide a good description of the observed properties (Chen et al., 1995).

The observed current through alm-BAPHDA channels is the sum of that carried by cations and anions through the channel. If these fluxes are assumed not to interact, then the Nernst-Planck equation can be used to describe each flux, and the total current is simply the sum of the two. Interaction between ions is accounted for, albeit not explicitly, in the calculation of the electrostatic profiles for cations and anions in the pore, as described above. Calculated electrostatic potentials were combined with a linear expression for the applied voltage drop across the membrane in calculating the integral in the denominator of the Nernst-Planck current equation (Eq. 1). The calculated electrostatic profile is one-dimensional. We assume, for simplicity, that the potentials are constant over the cross section of the pore (Levitt, 1991a). As discussed above, the Poisson-Boltzmann calculations are likely to give relative electrostatic energies more reliably than absolute ones, because information on effective dielectric constants is lacking. A variable parameter was therefore inserted to permit weighting of the magnitude of the channel electrostatic profile with respect to the (linear) applied field term. This factor was a fitted parameter; the calculated electrostatic potentials seem to overestimate the potentials required to fit the *I-V* curves by a factor of ~2.

Fig. 8 shows the *I-V* relationship calculated for alm-BAPHDA in 1 M KCl. Total current as well as the individual contributions of cation flux and anion flux are shown. Rectification of the total current in the same direction as that observed experimentally is clearly evident. The model predicts that at positive voltages in 1 M KCl, most of the current is carried by cations. This prediction is consistent with macroscopic measurements of alamethicin channel selectivity in which channels are primarily open in the "normal" orientation (Hall et al., 1984; Eisenberg et al., 1973).

Current-voltage relationships were then calculated for a series of ionic strengths by substituting the corresponding electrostatic profiles (calculated with ϵ(peptide) = 2, ϵ(solution) = 78) into Eq. 6. Importantly, the same correction factor (k) was used for the entire family of calculated *I-V* curves, so that differences in these curves faithfully reflect differences in the calculated profiles as a function of ionic strength. The correction factor compensates somewhat for the lack of experimental information about the channel molecularity; an octameric channel, for instance, would be expected to exhibit a different balance between the magnitude of the applied potential and the calculated electrostatic profile.

I-V curves for different ionic strengths were thus calculated entirely independently of any information about the corresponding experimental *I-V* relationships. The calculated curves were simply multiplied by a common (constant) factor to achieve the best visual fit with the experimental curves shown in Fig. 9. Given the relative simplicity of the model, the agreement between predicted and experimental curves is very good. There is (surprisingly) semiquantitative agreement between the calculated currents and those observed. A value of D of 2×10^{-5} cm^2 s^{-1} for ions in the pore is probably an overestimate (Breed et al., 1996,

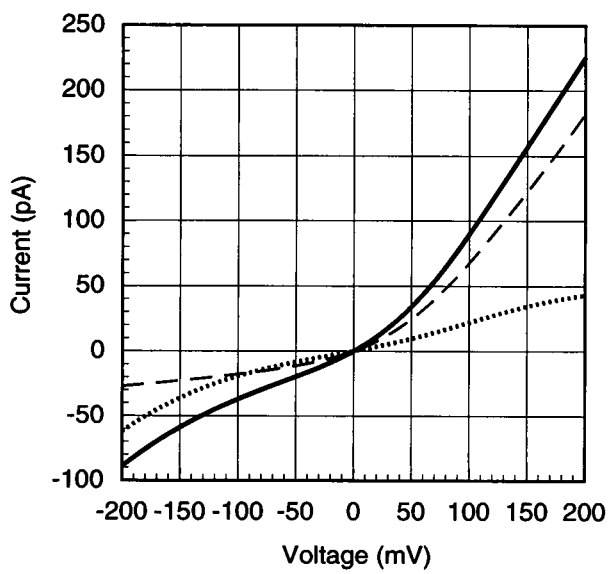

FIGURE 8 Calculated *I-V* curve, using Eq. 6 and the electrostatic potential profile calculated for 1 M KCl. ——, Total current; – – –, current carried by cations; ·····, current carried by anions. For details of the calculation, see Materials and Methods.

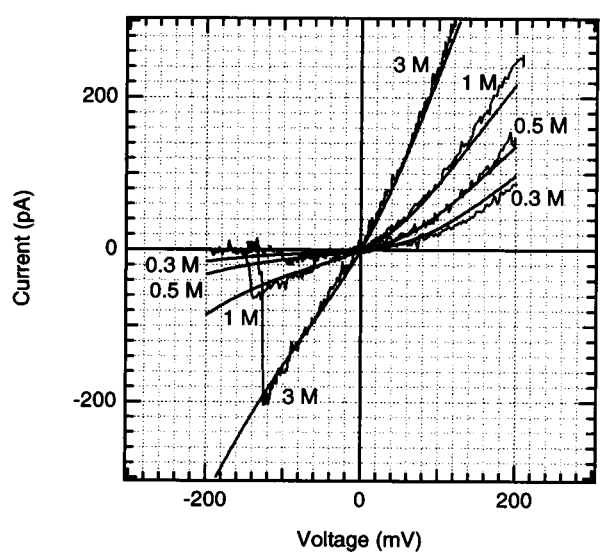

FIGURE 9 *I-V* curves calculated using the potential profiles in Fig. 7. Calculated curves are shown as solid smooth lines superimposed on experimental *I-V* curves obtained with a series of different KCl concentrations (as indicated).

1997), so that other estimated parameters (e.g., the effective area of the channel) are perhaps too small. Nevertheless, it appears that the models shown are sufficient to account qualitatively for the observed properties of alamethicin channels. In particular, the asymmetrical shape of the electrostatic profile (i.e., there is an energy well for cations toward the C-terminus and a barrier toward the N-terminus) predicts rectification in the correct direction. As the ionic strength increases, shielding of peptide dipoles diminishes the electrostatic contribution of the channel itself to the field, so that ions experience mainly the applied (linear) voltage gradient, and a more linear *I-V* curve results (Fig. 9).

We intend to further test the applicability of these models of alamethicin channels by studying the effect of mutations in the pore on selectivity and conductance.

REFERENCES

Barranger-Mathys, M., and D. S. Cafiso. 1996. Membrane structure of voltage-gated channel forming peptides by site-directed spin-labeling. *Biochemistry.* 35:498–505.

Begenisich, T. 1994. Permeation properties of cloned K^+ channels. *In* Handbook of Membrane Ion Channels. C. Peracchia, editor. Academic Press, San Diego.

Bek, S., and E. Jakobsson. 1994. Brownian dynamics study of a multiply occupied cation channel: application to understanding permeation in potassium channels. *Biophys. J.* 66:1028–1038.

Biggin, P. C., J. Breed, H. S. Son, and M. S. P. Sansom. 1997. Simulation studies of alamethicin bilayer interactions. *Biophys. J.* 72:627–636.

Boheim, G., W. Hanke, and G. Jung. 1983. Alamethicin pore formation: voltage-dependent flip-flop of α-helix dipoles. *Biophys. Struct. Mech.* 9:181–191.

Breed, J., P. C. Biggin, I. D. Kerr, O. S. Smart, and M. S. P. Sansom. 1997. Alamethicin channels: modelling via restrained molecular dynamics simulations. *Biochim. Biophys. Acta.* (in press).

Breed, J., R. Sankararamakrishnan, I. D. Kerr, and M. S. P. Sansom. 1996. Molecular dynamics simulations of water within models of ion channels. *Biophys. J.* 70:1643–1661.

Breed, J., and M. S. P. Sansom. 1994. Alamethicin channels modelled by simulated annealing and molecular dynamics. *Biochem. Soc. Trans.* 22:157S.

Cafiso, D. S. 1994. Alamethicin: a peptide model for voltage gating and protein-membrane interactions. *Annu. Rev. Biophys. Biomol. Struct.* 23:141–165.

Chen, D., P. Kienker, J. D. Lear, and R. S. Eisenberg. 1995. PNP theory fits current-voltage (IV) relations of a synthetic channel in 7 solutions. *Biophys. J.* 68:A370.

Cooper, K., E. Jakobsson, and P. Wolynes. 1985. The theory of ion transport through membrane channels. *Prog. Biophys. Mol. Biol.* 46: 51–96.

Davis, M. E., J. D. Madura, B. A. Luty, and J. A. McCammon. 1991. Electrostatics and diffusion of molecules in solution: simulations with the University of Houston Brownian dynamics program. *Comput. Phys. Comm.* 62:187–197.

Eisenberg, M., J. Hall, and C. A. Mead. 1973. The nature of the voltage-dependent conductance induced by alamethicin in black lipid membranes. *J. Membr. Biol.* 14:143–176.

Gordon, L. G. M. 1973. Ion Transport via Alamethicin Channels. *In* Drugs and Transport Processes. B. A. Callingham, editor. Macmillan, New York.

Gordon, L. G. M., and D. A. Haydon. 1972. The unit conductance channel of alamethicin. *Biochim. Biophys. Acta.* 255:1014–1018.

Gutman, M., Y. Tsfadia, A. Masad, and E. Nachliel. 1992. Quantitation of physical-chemical properties of the aqueous phase inside the PhoE ionic channel. *Biochim. Biophys. Acta.* 1109:141–148.

Hall, J. E., I. Vodyanoy, T. M. Balasubramanian, and G. R. Marshall. 1984. Alamethicin: a rich model for channel behavior. *Biophys. J.* 45:233–248.

Hille, B. 1992. Ionic Channels of Excitable Membranes, 2nd Ed. Sinauer Associates, Sunderland, MA.

Kerr, I. D., R. Sankararamakrishnan, O. S. Smart, and M. S. P. Sansom. 1994. Parallel helix bundles and ion channels: molecular modelling via simulated annealing and restrained molecular dynamics. *Biophys. J.* 67:1501–1515.

Kienker, P. K., W. F. Degrado, and J. D. Lear. 1994. A helical-dipole model describes the single-channel current rectification of an uncharged peptide ion channel. *Proc. Natl. Acad. Sci. USA.* 91:4859–4863.

Kienker, P. K., and J. D. Lear. 1995. Charge selectivity of the designed uncharged peptide ion channel Ac-$(LSSLLSL)_3$-$CONH_2$. *Biophys. J.* 68:1347–1358.

Latorre, R., and O. Alvarez. 1981. Voltage-dependent channels in planar lipid membranes. *Physiol. Rev.* 77–150.

Levitt, D. G. 1985. Strong electrolyte continuum theory solution for equilibrium profiles, diffusion limitation, and conductance in charged ion channels. *Biophys. J.* 48:19–31.

Levitt, D. G. 1986. Interpretation of biological ion channel flux data: reaction rate versus continuum theory. *Annu. Rev. Biophys. Biophys. Chem.* 15:29–57.

Levitt, D. G. 1991a. General continuum theory for multiion channel. I. Theory. *Biophys. J.* 59:271–277.

Levitt, D. G. 1991b. General continuum theory for multiion channel. II. Application to acetylcholine channel. *Biophys. J.* 59:278–288.

Mak, D. D., and W. W. Webb. 1995a. Molecular dynamics of alamethicin transmembrane channels from open-channel current noise analysis. *Biophys. J.* 69:2337–2349.

Mak, D. D., and W. W. Webb. 1995b. Two classes of alamethicin transmembrane channels: molecular models from single channel properties. *Biophys. J.* 69:2323–2336.

Molle, G., J. Y. Dugast, G. Spach, and H. Duclohier. 1996. Ion channel stabilization of synthetic alamethicin analogs by rings of inter-helix H-bonds. *Biophys. J.* 70:1669–1675.

North, C. L., M. Barranger-Mathys, and D. S. Cafiso. 1995. Membrane orientation of the N-terminal segment of alamethicin determined by solid-state ^{15}N-NMR. *Biophys. J.* 69:2392–2397.

Sansom, M. S. P. 1993a. Alamethicin and related peptaibols-model ion channels. *Eur. Biophys. J.* 22:105–124.

Sansom, M. S. P. 1993b. Structure and function of channel-forming peptaibols. *Q. Rev. Biophys.* 26:365–421.

Schultz, S. G. 1980. Basic Principles of Membrane Transport. Cambridge University Press, Cambridge.

Seoh, S., and D. Busath. 1993. The permeation properties of small organic cations in gramicidin channels. *Biophys. J.* 64:1017–1028.

Smart, O. S., J. M. Goodfellow, and B. A. Wallace. 1993. The pore dimensions of gramicidin A. *Biophys. J.* 65:2455–2460.

Taylor, R. J., and R. de Levie. 1991. "Reversed" alamethicin conductance in lipid bilayers. *Biophys. J.* 59:873–879.

Unwin, N. 1995. Acetylcholine receptor channel imaged in the open state. *Nature.* 373:37–43.

Vodyanoy, I., J. E. Hall, and T. M. Balasubramanian. 1983. Alamethicin-induced current-voltage curve asymmetry in lipid bilayers. *Biophys. J.* 42:71–82.

Woolley, G. A., R. M. Epand, I. D. Kerr, M. S. P. Sansom, and B. A. Wallace. 1994. Alamethicin-pyromellitate: an ion-activated channel-forming peptide. *Biochemistry.* 33:6850–6858.

Woolley, G. A., and B. A. Wallace. 1992. Model ion channels: gramicidin and alamethicin. *J. Membr. Biol.* 129:109–136.

You, S., S. Peng, L. Lien, J. Breed, M. S. P. Sansom, and G. A. Woolley. 1996. Engineering stabilized ion channels: covalent dimers of alamethicin. *Biochemistry.* 35:6225–6232.